

filled states and the next higher empty conduction band. The major features of the previously identified absorption from the deeper oxygen $2p$ bands do not change, although relatively small changes in the energy location and polarization dependence of the absorption peaks were observed.

A more detailed comparison of the absorption due to the extra d electron per vanadium ion at temperatures below 68°C to that expected on the basis of present theories of the metal-semiconductor transition is inconclusive. Although it is clear that a simple band picture is qualitatively consistent not only with the measured optical properties but also the metal-semiconductor transition, there are indications that such a model may be a considerable oversimplification. In addition, a model based on the assumption that the extra d electron per vanadium ion is trapped in a local-

ized level has equal qualitative consistency with the data. It is more likely that neither model is completely correct. Since the extra d electron per vanadium ion is largely responsible for the crystal forces which result in the distorted, monoclinic structure at temperatures below 68°C , effects in optical absorption similar to those observed in the F and V_k centers of the alkali halides are expected to occur.

ACKNOWLEDGMENTS

The authors wish to thank H. J. Guggenheim and D. H. Hensler for supplying the VO_2 crystals and films studied in this work, and G. E. Mahoney for making many of the measurements. Helpful comments and suggestions from G. E. Smith and J. Brews, and very useful discussions about the band structure of VO_2 with L. Mattheiss are also gratefully acknowledged.

Electroreflectance Studies of InAs, GaAs, and (Ga,In)As Alloys*

E. W. WILLIAMS†

Royal Radar Establishment, Malvern, Worcestershire, England

AND

VICTOR REHN

Michelson Laboratory, China Lake, California 93555

(Received 2 October 1967; revised manuscript received 5 April 1968)

The technique of electroreflectance was applied to the study of epitaxial (Ga, In)As alloys. Two experimental methods were used and their relative merits are discussed. The $\Gamma_{15}-\Gamma_1$ and $\Lambda_3-\Lambda_1$ transitions and their spin-orbit splittings were investigated as functions of alloy composition. The spin-orbit splitting at $k=0$ for InAs at room temperature was measured directly as 0.446 ± 0.008 eV. The electroreflectance linewidth changes by a factor of 4 for the $\Gamma_{15}-\Gamma_1$ series between InAs and GaAs. The broadening is discussed in terms of mechanisms such as field inhomogeneity and light-hole lifetime for the InAs-rich alloys. The deviations from a linear concentration dependence that were observed for all of the energy gaps were almost all identical and were related to the virtual-crystal model. Transitions below the fundamental gap were correlated with impurities by the use of photoluminescence measurements on the same samples.

I. INTRODUCTION

THE energy-band structures of GaAs and InAs have been calculated theoretically^{1,2} and a large number of experimental results have yielded band-structure parameters. Of the experimental techniques available, only optical techniques allow the experimenter to study a wide range of interband energy, and

conventional normal-incidence reflectivity and optical-absorption measurements have been made on these materials previously. Woolley and Blazey³ studied the $\Lambda_3-\Lambda_1$, $\Gamma_{15c}-\Gamma_{15e}$, and X_5-X_1 interband transitions by normal-incidence reflectance in polycrystalline samples of (Ga,In)As alloys and concluded that the energies of these transitions vary linearly with composition. Jones⁴ subsequently used the same technique and found that the $\Lambda_3-\Lambda_1$ transition energy showed a nonlinear dependence on composition at the InAs end of the alloy series. Optical-absorption studies of the fundamental absorption region in these alloys have been

* A preliminary version of this paper was given at the New York A. P. S. Meeting: Bull. Am. Phys. Soc. **12**, 101 (1967).

† The experimental work described here was performed while this author was with Texas Instruments Incorporated, Dallas, Tex. 75222.

¹ Marvin L. Cohen and T. K. Bergstresser, Phys. Rev. **141**, 789 (1966).

² F. H. Pollak, C. W. Higginbotham, and M. Cardona, J. Phys. Soc. Japan Suppl. **21**, 20 (1966).

³ J. C. Woolley and K. W. Blazey, J. Phys. Chem. Solids **25**, 713 (1964).

⁴ C. E. Jones, Appl. Spectry. **20**, 161 (1966).

reported in three publications,⁵⁻⁷ and all conclude that the fundamental absorption threshold $\Gamma_{15}-\Gamma_1$ varies nonlinearly with composition, but all of these studies disagree on the shape of this phase curve.

This paper reports the application of the Seraphin effect (electroreflectance) to the study of the $\Gamma_{15}-\Gamma_1$ (fundamental optical threshold) and the $\Lambda_3-\Lambda_1$ transitions, and their spin-orbit split-off companions in high-quality, epitaxial single crystals of (Ga,In)As alloys, and in GaAs and InAs single crystals. We also report combined electroreflectance and photoluminescence studies of impurity-associated transitions observed below the fundamental absorption threshold. Optical-absorption studies of the fundamental absorption threshold on the same crystals are reported and compared with the electroreflectance spectra. The first direct experimental measurements of the valence band spin-orbit splitting term, Δ_0 , in InAs is reported. Surface-barrier electroreflectance (SBE) spectra taken by the Seraphin technique and by the technique of Shaklee *et al.* on the same samples are compared, and a discussion is given of the merits and limitations of each.

The study of the reflectivity of semiconductor alloys has proved to be very useful in analyzing band-structure changes with change in the fundamental gap from semiconductor to semiconductor, and in verifying the relationship of the interband transitions in the constituent compounds. For example, in the Ga(As,P) system, normal incidence reflectance techniques were used to verify the $\Gamma_{15c}-\Gamma_{15c}$ transition in GaP. A new peak observed in GaP at 4.83 eV was followed through the alloy system to 4.40 eV in GaAs.⁸ Strong evidence developed that this could be assigned to $\Gamma_{15c}-\Gamma_{15c}$ transition, or a small region of the Brillouin zone about this.⁸ Low-temperature measurements^{9,10} and electroreflectance measurements¹¹ on the Ga(As,P) system confirmed this identification. A similar confirmation of the $\Lambda_3-\Lambda_1$ transition in GaP resulted from alloy studies, and cleared up earlier confusion that had resulted from temperature and pressure dependences.⁸⁻¹²

The theoretical relationship between one-electron band structures of crystals and the electronic structure of alloys was first considered by Nordheim,¹³ who intro-

duced the "virtual-crystal" model. In this model the actual *nonperiodic* potential is replaced by one representing a periodic crystal with an *average* occupancy of lattice sites and an average (scaled) interatomic spacing. Muto¹⁴ showed that in the case of small alloy concentrations this approximation gives energy levels accurate to first order in perturbation theory. Parmenter¹⁵ considered the effect of higher-order perturbations and then offered corrections to the virtual-crystal model, which account for both the effects of random fluctuations in the potential and those of changes in the wave function which do not scale with the lattice constant.¹⁶ This definitive work provides a firm basis for the study of the band structure of crystals through their alloys, showing that in spite of the nonperiodic nature of the potential, a one-electron band structure with k as quantum number is a good description of the electronic structure of alloys, and that the principal departures from this picture are expected to be the existence of localized electronic states and the "tailing" of states into the forbidden energy region of the one-electron band structure. Subsequently, Mattuck¹⁷ showed the effects of long- and short-range order, of clustering, and of tailing on the alloy band structure, and Smith¹⁸ showed the effect of a random environment on the spin-orbit interaction.

With this background picture, one expects that one-electron interband optical absorptions, and related effects, in alloys should be observable and interpretable much as in perfect crystals. The departures to be expected are in the tailing of states, or the "fuzzing out" of the interband absorption thresholds, and in the effects of localized electronic states. Experiments so far show neither of these effects. Absorption thresholds observed by us and by others are just as sharp as in the pure compound crystals. Electroreflectance structural widths at the fundamental and higher thresholds show *no* appreciable alloy broadening. Effects we have observed which might be attributed to alloying are in the impurity-associated phenomena and in the composition dependences of spin-orbit splitting. These are discussed more thoroughly in Sec. VI.

In Sec. II are described the sample growth, analysis, surface preparation, and SBE techniques of Seraphin,¹⁹⁻²² using a SnO₂ coated glass or quartz electrode,

⁵ M. S. Abrahams, R. Braunstein, and F. D. Rosi, *J. Phys. Chem. Solids* **10**, 204 (1959).

⁶ J. C. Woolley, C. M. Gillett, and J. A. Evans, *Proc. Phys. Soc. (London)* **77**, 700 (1961).

⁷ E. F. Hockings, I. Kudman, T. E. Seidel, C. M. Schmelz, and E. F. Steigmeier, *J. Appl. Phys.* **37**, 2879 (1966).

⁸ T. K. Bergstresser, Marvin L. Cohen, and E. W. Williams, *Phys. Rev. Letters* **15**, 662 (1965).

⁹ J. C. Woolley, A. G. Thompson, and M. Rubinstein, *Phys. Rev. Letters* **15**, 670 (1965); **15**, 768(E) (1965).

¹⁰ A. G. Thompson, J. C. Woolley, and M. Rubinstein, *Can. J. Phys.* **44**, 2927 (1966).

¹¹ A. G. Thompson, M. Cardona, K. L. Shaklee, and J. C. Woolley, *Phys. Rev.* **146**, 601 (1966).

¹² E. W. Williams and C. E. Jones, *Solid State Commun.* **3**, 195 (1965).

¹³ L. Nordheim, *Ann. Physik* **9**, 607 (1931); **9**, 641 (1931).

¹⁴ T. Muto, *Sci. Papers Inst. Phys. Chem. Res. (Tokyo)* **34**, 377 (1938).

¹⁵ R. H. Parmenter, *Phys. Rev.* **97**, 587 (1955).

¹⁶ R. H. Parmenter, *Phys. Rev.* **99**, 1759 (1955).

¹⁷ R. D. Mattuck, *Phys. Rev.* **127**, 738 (1962).

¹⁸ David Young Smith, *Phys. Rev.* **137**, A574 (1965).

¹⁹ B. O. Seraphin, in *Proceedings of the Seventh International Conference on The Physics of Semiconductors, Paris, 1964* (Academic Press Inc., New York, 1964), p. 165.

²⁰ B. O. Seraphin and R. B. Hess, *Phys. Rev. Letters* **14**, 138 (1965).

²¹ B. O. Seraphin, R. B. Hess, and N. Bottka, *J. Appl. Phys.* **36**, 2242 (1965).

²² B. O. Seraphin, *Phys. Rev.* **140**, A1716 (1965).

TABLE I. Description of samples.

Sample No.	Orient. surface	Type	Carrier ^a concn. (cm ⁻³)	Comp. ^b (mole % GaAs)	Thickness ^c (μ)	Meas. ^d reported
Various	100 and 111	<i>n</i> and <i>p</i>	Various	100	5-1000 ^e	PL, EE, A
7487-1-544-4	100	<i>n</i>	5.6×10^{16}	84	7.3	CGE
7487-22-553	100	<i>p</i> ^f	8×10^{17}	83	5.2	EE
6998-150-509	100	<i>n</i>	1×10^{17}	80	11.6	EE, CGE, PL, A
7487-100-544	100	<i>n</i>	1.1×10^{18}	75	2.3	EE
6998-18-435	100	<i>n</i>	7×10^{15}	79	59	CGE
8071-68-571	100	<i>n</i>	1×10^{16}	60	5.2	CGE, A
7487-107-544	100	<i>n</i>	7.4×10^{16}	44	8.1	CGE, A
8071-70-571	100	<i>n</i>	1×10^{16}	20	19	CGE, A
OW-80	111	<i>n</i>	5×10^{16}	0	1000 ^e	CGE
OW-81	111	<i>n</i>	9×10^{16}	0	1000 ^e	CGE

^a Carrier concentration measured by Hall effect.

^b Composition measured by an x-ray technique. See text and Ref. 27.

^c Thickness measured by the bevel-stain technique. All substrates *n*-type GaAs, Te doped, approximately 1×10^{18} .

^d PL = photoluminescence at 20°K, EE = electrolyte-electrode electroreflectance, CGE = conducting-glass-electrode electroreflectance, A = optical absorption.

^e Bulk material samples.

^f Cadmium doped.

and of Shaklee, Pollak, and Cardona,²³ using an electrolyte electrode. These SBE techniques are compared, and results obtained by each from the same sample are shown. In Sec. III the results are given of optical-absorption measurements and SBE measurements at the fundamental absorption edge $\Gamma_{15}-\Gamma_1$ and its spin-orbit split-off component. The spin-orbit splitting factor Δ_0 for this transition is given versus composition,²⁴ and the change in the SBE line shapes with composition are also shown. In Sec. IV we describe our experimental results in the vicinity of the $\Lambda_3-\Lambda_1$ transition, where our SBE energies depart considerably from those of the reflectivity peaks reported in Refs. 3 and 4. Section V describes combined electroreflectance and photoluminescence studies of the impurity-associated transitions observed below the fundamental absorption threshold. Correlated signals observed by these two techniques show conclusively the relationship of the impurity-associated signal to the fundamental interband optical structure. In the concluding section, Sec. VI, discussions are presented of the physical origins of the SBE line-shape changes with composition, the dependence of the spin-orbit splitting term on composition, the discrepancy between the SBE measurements and the reflectance measurements of the $\Lambda_3-\Lambda_1$ transitions in terms of the virtual-crystal model and its corrections, and the impurity-associated phenomena.

²³ K. L. Shaklee, F. H. Pollak, and M. Cardona, Phys. Rev. Letters **15**, 883 (1965).

²⁴ This measurement was presented at the American Physical Society Meeting in New York [Bull. Am. Phys. Soc. **12**, 101 (1967)]. After submission of this manuscript for publication, a magneto-electroreflectance observation of $\Gamma_7-\Gamma_6$ by C. R. Pidgeon, S. H. Groves, and J. Feinleib [Solid State Commun. **5**, 677 (1967)] came to our attention, from which they deduce $\Delta_0 = 0.38 \pm 0.01$ eV. In a private communication Dr. Pidgeon points out that although he finds an electroreflectance extremum at 0.850 eV ($H=0$, $T=1.4^\circ\text{K}$) he has no justification for associating this point with the $\Gamma_7-\Gamma_6$ threshold. Similarly, we find an electroreflectance extremum at 0.74 eV (90°K), but its behavior with temperature and composition does not support its assignment as the $\Gamma_7-\Gamma_6$ threshold. Further studies are required to settle this puzzle.

II. EXPERIMENTAL DISCUSSION

A. Sample Growth, Analysis, and Surface Preparation

Only single-crystal samples were used. The epitaxial alloy samples, grown on (100) tellurium-doped GaAs substrates, were of uniform thickness in the range 2-60 μ . (See Table I.) Growth was in an open-reactor-tube, vapor-phase deposition system, as described in detail elsewhere.²⁵ The (100) orientation was chosen for the alloys in preference to the (111) orientation because of the faster growth rate and the smaller rate of incorporation of donor impurities during growth.²⁶ GaAs and InAs samples were grown either epitaxially or from the melt. The carrier concentrations of all samples were in the range 7×10^{15} - 1×10^{18} carriers/cm³, and all samples but one were *n* type.

The average composition of the alloy samples was determined by measuring the angular separation $\Delta\theta$ of the (400) Bragg reflections of the GaAs substrate and the (Ga,In)As layer.²⁷ The accuracy of this measurement depends on the accuracy of measurement of $\Delta\theta$ and on the homogeneity of the composition of the layer. Therefore, in alloys containing less than 20 mole % InAs the accuracy of composition determination was reduced because of the smallness of $\Delta\theta$. Below 7 mole % InAs the reflections could not be resolved. The accuracy in $\Delta\theta$ is not as great for the (400) reflection as for the (333) reflection used for (111)-face samples, because of the smaller $\Delta\theta$ and the lower intensity of the reflected x rays. The homogeneity of the alloys was checked using reflectivity, optical absorption, and x-ray methods as described previously.^{28,29}

²⁵ R. W. Conrad, P. L. Hoyt, and D. D. Martin, J. Electrochem. Soc. **114**, 164 (1967).

²⁶ F. V. Williams, J. Electrochem. Soc. **111**, 886 (1964).

²⁷ J. K. Howard and R. D. Dobrott, J. Electrochem. Soc. **113**, 567 (1966).

²⁸ R. W. Conrad, C. E. Jones, and E. W. Williams, J. Electrochem. Soc. **113**, 287 (1966).

²⁹ E. W. Williams, R. H. Cox, R. D. Dobrott, and C. E. Jones, J. Electrochem. Tech. **4**, 479 (1966).

The samples were found to be homogeneous within the limits of resolution of the analytical measurements, estimated as ± 3 mole %.

The epitaxial surfaces were normally very smooth, though occasionally small pyramidal hillocks were present. Samples were sometimes polished with 0.3- μ alumina to remove surface "haze" and then always lightly etched with either a 2% solution of bromine in methanol, or an equal mixture of concentrated HCl and HNO₃. As-grown epitaxial alloy surfaces were not used since they sometimes give anomalous reflectivity results caused by the reactor shut-down procedure.^{28,29} Samples that were only mechanically polished show that broad reflectivity peaks shifted considerably in energy. This shift was random in magnitude and direction, indicative of surface strain produced by the mechanical polishing.

B. SBE with the Conducting-Glass-Electrode Technique

This is the original modulated reflectance technique, due to Seraphin and co-workers.¹⁹⁻²² The conducting sample is made one electrode of a parallel plate capacitor, a conducting glass window the other, and the sample surface barrier, covered with a thin insulating film, is the dielectric. As the voltage across the capacitor varies, the space charge in the sample surface barrier region charges, and the electric field due to this space charge is caused to vary. Thus by application of an alternating voltage to the capacitor, the electric field in the surface barrier region of the sample is modulated synchronously. Depending upon the material, modulation frequencies up to 10⁴ Hz or more may be used, with 100-600 V rms sufficient to produce large field swings. In these measurements 1-5 kHz was used, typically with 300-500 V rms.

C. SBE with the Electrolyte-Electrode Technique

In this technique, due to Shaklee, Pollak, and Cardona,^{11,23,30} the sample is made the negative electrode of an electrolytic cell. The electrolyte used was a 0.1 *N* solution of KCl in H₂O, and the positive electrode was a platinum wire. The cell is biased in the blocking direction with a dc voltage of about 1 V, and an ac modulating voltage was superimposed on the dc bias. The ac frequency range possible is 10-2000 Hz; the frequency used was usually about 200 Hz, where the signal-to-noise ratio was best. The ac voltage was monitored on an oscilloscope, and care was taken not to "over-drive" the cell with too high an ac voltage. The reflected monochromatic light from the sample surface was detected with a suitable photomultiplier, and a servoloop was arranged to keep the dc output constant. Hence the lock-in amplifier output gave $\Delta R/R$ directly.

³⁰ M. Cardona, K. L. Shaklee, and F. H. Pollak, Phys. Rev. **154**, 696 (1967).

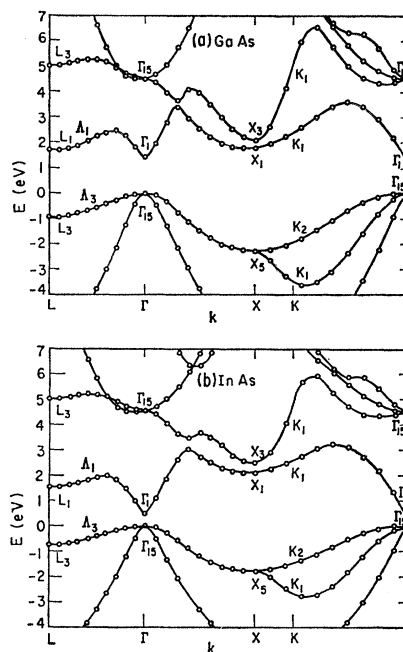


FIG. 1. Pseudopotential band structures for (a) GaAs, (b) InAs, from Ref. 1. Compare also the GaAs band structure of Ref. 29.

The servoloop was arranged as follows: The difference between a reference voltage and the dc photomultiplier output voltage was amplified and used to program the power supply for the 500-W tungsten source lamp. Hence when the reflected light intensity decreased slightly, the lamp intensity was caused to increase proportionately. This servoloop and its applications will be described more fully elsewhere.³¹

D. Comparison of SBE Techniques

Fundamentally the two electroreflectance methods described above are very similar. Both are SBE methods, relying on the space charge in the surface barrier region of the sample to provide the electric field. Since this field must be modulated, conductivity of the sample is required or else the space charge in the sample could not be varied.³² In this requirement the conducting glass electrode (CGE) technique seems superior, since sample resistivities up to 1000 Ω cm have proven usable, while the electrolyte electrode (EE) technique seems limited to resistivities less than one Ω cm. This is probably due to the very much lower capacity in the former barrier than in the latter.

Both methods require a transparent electrode, which necessarily limits the wavelength transmission range. In CGE the SnO₂ layer prevents measurements at photon energies above 4.5 eV, but does not limit the low energy transmission (until perhaps 0.12 eV). In

³¹ E. W. Williams and D. V. Parham, Rev. Sci. Inst. **39**, 369 (1968).

³² See last paragraph of Sec. II.

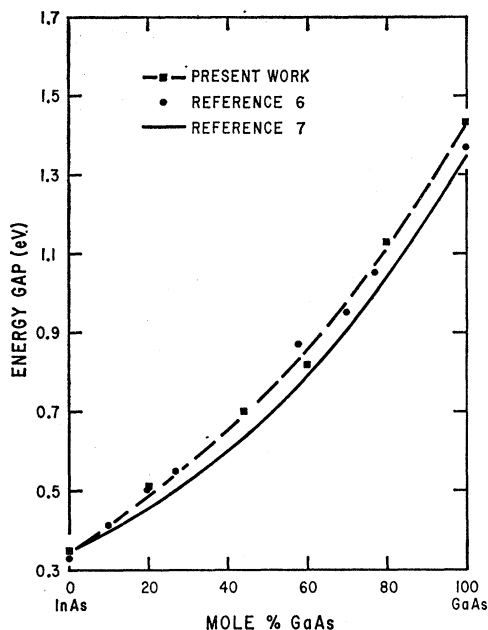


Fig. 2. Fundamental energy gap ($\Gamma_{15}-\Gamma_1$) versus composition from optical-absorption measurements.

our apparatus the low-energy limit, due to scattered light from the monochromator and failing detector sensitivity (PbS), was about 0.45 eV. In the EE technique the water in the electrolyte limits the transmission of the low-energy light to 1.2 eV unless special precautions are taken to reduce the optical path length in the electrolyte. With a very thin layer of electrolyte, transmission down to 0.7 eV is obtained.^{33,34} The high energy cut-off of the EE technique is nearly 6 eV.

The temperature limitations of the EE technique are more severe, because 0.1 *N* KCl in H₂O electrolyte freezes about 273°K. The use of propyl alcohol instead of water reduces this limitation to 146°K.²³ With the CGE method, experiments have been performed from 80 to 373°K^{21,35} and there is no reason to believe that experiments could not be performed from the He temperature range to still higher temperatures.

In the EE method irregularly shaped samples can be used, and surface irregularities such as hillocks are of no hindrance, besides degrading the optical performance slightly. CGE requires reasonably flat sample surfaces, since, if the capacitor is not constructed carefully, interference effects may produce false, large amplitude ΔR drifts, or hillocks may puncture the insulating layer. If mechanical motion is permitted between the sample surface and the SnO₂ electrode,

³³ M. Cardona, K. L. Shaklee, and F. H. Pollak, *Phys. Letters* **23**, 37 (1966).

³⁴ S. H. Groves, C. R. Pidgeon, and J. Feinleib, *Phys. Rev. Letters* **17**, 643 (1966).

³⁵ B. O. Seraphin, *J. Appl. Phys.* **37**, 721 (1966); *Proc. Phys. Soc. (London)* **87**, 239 (1966).

spurious sinusoidal variations of $\Delta R/R$ with wavelength will result from a synchronously vibrating interferometer effect.²¹

In the EE experiment a few drops of concentrated HCl in the electrolyte prevents the GaAs surface from becoming badly oxidized. Alternatively, alcohol can be used instead of water for materials which react with water or air, and the sample can be cleaved in the alcohol producing "fresh" surfaces for study.³⁶

A serious limitation of both SBE methods is the non-uniform nature of the electric field. This makes it impossible to apply field-effect theory quantitatively to understand the line shapes and field dependences. Another method, transverse electroreflectance,³⁷ overcomes this and other limitations, though it is applicable only to insulating samples ($\rho > 10^8 \Omega/\text{cm}$).

III. FUNDAMENTAL EDGE ($\Gamma_{15}-\Gamma_1$)

The smallest energy gap between the valence band and conduction band, the fundamental gap, lies at $k=(0,0,0)$, or Γ , in these materials, and is labeled $\Gamma_{15}-\Gamma_1$. (See Fig. 1.) The threshold energy for indirect transitions is 1.9 eV in GaAs, and is predicted to be 1.6 eV for $\Gamma_{15}-L_1$ in InAs.¹

The spin-orbit interaction at $k=0$ splits the Γ_{15} valence band into Γ_7 and Γ_8 bands of the double group. The separation Δ_0 of these for GaAs has been determined from measurements of the optical transitions $\Gamma_7-\Gamma_6$ and $\Gamma_8-\Gamma_6$ ³⁸ to be $0.35 \text{ eV} \pm 0.01 \text{ eV}$ ³⁹ and from intraband free-hole transitions below the energy gap to be 0.33 eV.⁴⁰ By electroreflectance, Seraphin³⁵ obtained $0.348 \pm 0.002 \text{ eV}$, and Cardona *et al.*³⁰ obtain 0.34 eV. In the case of InAs, Matossi and Stern⁴¹ have deduced 0.43 eV from intraband transition studies.

A. Absorption Results

The transmission curves measured for four epitaxial alloy samples indicated that the absorption edge was very steep and similar to that measured for the compounds. The room-temperature energy gap values E_g , obtained from the absorption measurements by the method of Woolley *et al.*,⁴² are plotted in Fig. 2. In the same figure are plotted the absorption results of Woolley *et al.*,⁶ made on single-phase directionally frozen solid specimens. Although the latter were polycrystalline, the E_g values for the alloys are in good agreement with the present measurements. Their E_g value for GaAs is 1.37 eV, somewhat lower than the

³⁶ M. Cardona, F. H. Pollak, and K. L. Shaklee, *Phys. Rev. Letters* **16**, 644 (1966).

³⁷ V. Rehn and D. S. Kyser, *Phys. Rev. Letters* **18**, 848 (1967).

³⁸ In the double-group notation appropriate to the representation of energy bands in the presence of spin-orbit interactions, Γ_1 becomes Γ_6 . See, for example, R. J. Elliott, *Phys. Rev.* **96**, 280 (1954).

³⁹ M. D. Sturge, *Phys. Rev.* **127**, 768 (1962).

⁴⁰ R. Braunstein, *J. Phys. Chem. Solids* **8**, 280 (1959).

⁴¹ F. Matossi and F. Stern, *Phys. Rev.* **111**, 472 (1958).

⁴² J. C. Woolley, C. M. Gillett, and J. A. Evans, *J. Phys. Chem. Solids* **16**, 138 (1960).

TABLE II. $\Gamma_{15}-\Gamma_1$ data summary.

Mole % GaAs	$\Gamma_{15}-\Gamma_1$ Peaks (eV)	Δ_0 (eV)	Method
0	...	0.796±0.004	CGE
0	0.350±0.004	...	A
20	...	0.908±0.004	CGE
20	0.509±0.004	...	A
44	0.677±0.007	1.022±0.013	CGE
44	0.704±0.004	...	A
60	0.821±0.006	...	A
80	1.128±0.003	1.470±0.003	CGE
80	1.129±0.002	1.471±0.004	EE
80	1.133±0.004	...	A
84	1.184±0.004	...	CGE
83	1.167±0.003	1.50 ±0.01	EE
100	1.416±0.003	1.755±0.003	CGE
100	1.429±0.003	1.77 ±0.01	EE
100	1.430±0.004	...	A

present value of 1.43 eV, but their InAs value of 0.33 eV is close to the present measurement, 0.35 eV. The E_g data of Hockings *et al.*⁷ are also plotted in Fig. 2, but those of Abrahams *et al.*⁵ are not presented since many of their alloys were inhomogeneous. Only the curve resulting from Hocking *et al.* measurements has been plotted; the individual points have been left off for the sake of clarity. The complete reason for this curve's falling below the other measurements in Fig. 2 is not known, but in part it must be related to the small absorption constant (100 cm^{-1}) which they selected for the energy-gap value. Since they deduced a smaller E_g for GaAs, it is perhaps not surprising that their E_g values for the alloys are small as well.

For GaAs, Sturge³⁹ has carefully deduced E_g from his absorption measurements, accounting for the effects of exciton formation and sample strain. His measurements were made from 10°K to room temperature, and at the latter temperature he finds $E_g = 1.435 \pm 0.003$ eV. This is slightly higher than the values reported from electroreflectance measurements: Seraphin, 1.42; Cardona *et al.*; 1.43, the present work, 1.43. Whether this tiny discrepancy has any bearing on exciton effects or may be explained in terms of lifetime and electric field broadening effects must await further low-temperature studies. For InAs, diamagnetic Landau effect experiments have yielded an $E_g = 0.360 \pm 0.002$ eV at room temperature.⁴³ This also is within experimental error of the value reported here, 0.35 eV.

B. Electroreflectance

Both techniques of SBE were applied, and the results were found to be very similar, as shown in Fig. 3 for an 80-mole % GaAs alloy. The structure and linewidth of both curves is similar to that observed in GaAs, and the low-energy negative peak at 1.128 eV is identified as the fundamental edge. Following the

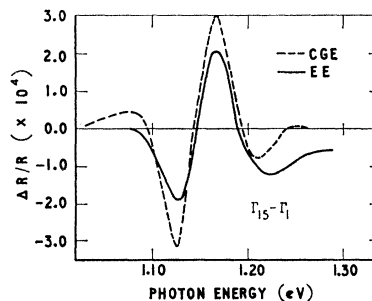


FIG. 3. A comparison of the $\Gamma_{15}-\Gamma_1$ structures observed by the two techniques of surface-barrier electroreflectance on the same 80 mole % GaAs sample. Experimental conditions: CGE technique: 300 V rms, 0 V dc, PbS detector; EE technique: 0.5 V ac, 1.2 V dc, PM detector. The EE structure below 1.10 eV is not accurate, due to electrolyte absorption.

edge are two or three Airy-function oscillations.^{44,45} Because of the similarity of the SBE results, no distinction will be made between them in the following. In Table II the results of both methods for the $\Gamma_{15}-\Gamma_1$ transitions have been tabulated.

In Fig. 4 are compared absorption and electroreflectance measurements made on the same samples. The results show an appreciable deviation from a linear dependence on concentration, though it is not as great as indicated by earlier absorption measurements.^{5,7} The main experimental error is in the composition measurements. This error ($\pm 4\%$) has been indicated by the error bar on the 60-mole % GaAs sample. The errors in the energy determination are very small and are indicated in Table II. The maximum departure from the straight line connecting InAs and GaAs occurs between 50- and 60-mole % GaAs, and is about 0.15 eV. This deviation is discussed further in the concluding section.

The spin-orbit component transition ($\Gamma_7-\Gamma_6$) has been plotted in Fig. 4. Its maximum deviation from the linear dependence is about 0.18 eV, and occurs at approximately the same composition. The change in the spin-orbit splitting Δ_0 of the valence band across the alloy system is shown in Fig. 4(b). The splitting remains approximately constant for the gallium-rich alloys and then increases rapidly at the InAs end. The value of Δ_0 for GaAs, 0.340 ± 0.004 eV, is slightly lower than that measured by Seraphin.³⁵ This value lies between the values found from previous absorption measurements, as mentioned above. Δ_0 for InAs has not been measured directly before, but the present value of 0.446 ± 0.008 is close to that deduced previously from intraband hold transitions, 0.43 eV. The present value is the difference between the $\Gamma_8-\Gamma_6$ energy (0.350 eV), as measured by absorption, and the $\Gamma_7-\Gamma_6$ energy (0.796 eV), as measured by electroreflectance. (As

⁴³ S. Zwerdling, B. Lax, and L. M. Roth, Phys. Rev. **108**, 1402 (1957).

⁴⁴ B. O. Seraphin and N. Bottka, Appl. Phys. Letters **6**, 134 (1965); Phys. Rev. **139**, A560 (1965); **145**, 628 (1966).

⁴⁵ J. C. Phillips, Phys. Rev. **146**, 584 (1966).

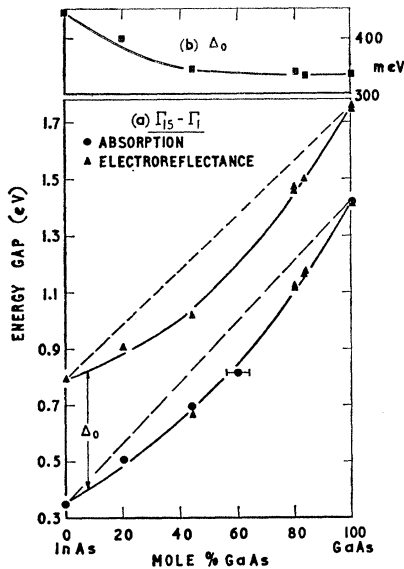


FIG. 4. The composition dependences of (a) the $\Gamma_{15}-\Gamma_1$ transitions in (Ga,In)As, and (b) the spin-orbit splitting factor Δ_0 . Both electroreflectance and optical-absorption data are represented.

mentioned previously CGE-technique electroreflectance measurements could not be made below 0.45 eV on the present equipment.)

An interesting line-shape change occurs across the alloy system, as a comparison of Fig. 5 with Fig. 3 shows. Figure 5 shows the spin-orbit split-off transition ($\Gamma_7-\Gamma_6$) in InAs and two InAs-rich alloys. The broad, structureless single-hump curve observed is in contrast to the $\Gamma_8-\Gamma_6$ structure shown in Fig. 3 for a GaAs-rich alloy. The spin-orbit split components $\Gamma_8-\Gamma_6$ and $\Gamma_7-\Gamma_6$ have always been observed to have identical line shapes, although the strength of $\Gamma_8-\Gamma_6$ is much greater. This lineshape change occurs about the same composition at which the Δ_0 -versus-composition curve flattens out. More will be said on this point in Sec. VI.

IV. SADDLE POINT $\Lambda_3-\Lambda_1$

The next higher interband threshold is an M_1 -type saddle point, which is spin-orbit split in the valence band. The exact locations in k space are uncertain,^{29,46} though it is generally agreed that they are in the $[111]$ directions, and closer to the Γ point than to the L point. Kane⁴⁷ has shown that the optical reflectance structure, from which the original critical-point identification was made, cannot be adequately understood by the critical-point contributions alone. Instead, contributions to $\epsilon_2(\omega)$, which determines the reflectance structure in this range, must be taken from broad regions of k space over which the valence and conduc-

⁴⁶ M. Cardona, in *Proceedings of the Seventh International Conference on the Physics of Semiconductors, Paris, 1964* (Academic Press Inc., New York, 1965), p. 181.

⁴⁷ E. O. Kane, *Phys. Rev.* **146**, 558 (1966).

tion bands are approximately parallel. No such arguments have yet been shown to apply in electroreflectance, however, where the response is determined by the derivative of $\epsilon_2(\omega)$ with respect to electric field. Further remarks on this distinction are made in Sec. VI.

Previous normal-incidence reflectance measurements for these transitions in (Ga,In)As are shown in Fig. 6. The measurements of Woolley and Blazey³ show an approximate linear dependence on composition for these transitions. The split-off transition data are not shown here, but behave similarly. The reflectivity measurements of Jones⁴ were made on samples similar to ours, so it would be expected that the electroreflectance measurements should confirm these. However, the deviation from linear composition dependence at just the InAs end observed by Jones was not duplicated by the SBE measurements, as Fig. 6 shows. Apart from InAs the SBE measurements for the alloys fall below the reflectance values. The SBE points fall on a smooth curve with a maximum deviation of 0.15 eV from linearity at about the 60-mole % GaAs composition. This deviation is a large fraction at the total energy change from InAs to GaAs, 0.38 eV.

The composition dependence of the two components of this spin-orbit split doublet are identical within experimental accuracy.⁴⁸ This is illustrated in Fig. 7(a). Plotted in Fig. 7(b) is the spin-orbit splitting term Δ_1

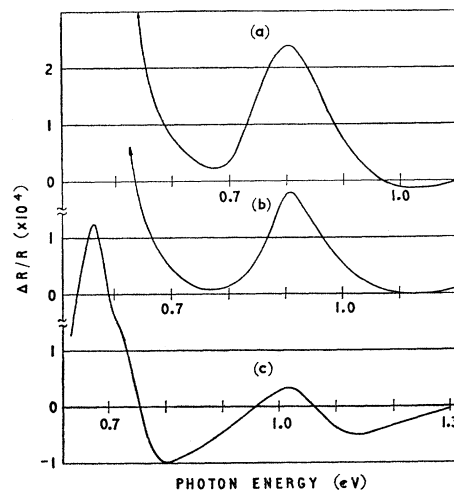


FIG. 5. Electroreflectance spectral shapes for InAs and two In-rich alloys. Peak shown is the spin-orbit split-off peak $\Gamma_7-\Gamma_6$. Except for the 44 mole % GaAs spectrum, the main $\Gamma_{15}-\Gamma_1$ peak, $\Gamma_8-\Gamma_7$, is off scale at lower energy. Spectra taken with 500 V rms, 0 V dc, modulation frequency 1.0–2.5 KHz, and optical resolution ≤ 10 meV.

⁴⁸ Under the spin-orbit interaction the single-group representation Λ_3 becomes the double-group representation $\Lambda_4+\Lambda_5+\Lambda_6$, while Λ_1 becomes Λ_6 . According to Cardona *et al.* (Ref. 30) the Λ_3 triplet splits into two levels of which the lower is Λ_6 and the upper is $\Lambda_4+\Lambda_5$. Hence what we refer to as the spin-orbit split-off structure is that due to the $\Lambda_{6v}-\Lambda_{6c}$ transition, while the larger, lower-energy $\Lambda_3-\Lambda_1$ structure is due to $(\Lambda_4+\Lambda_5)_v-\Lambda_{6c}$.

TABLE III. Λ_3 - Λ_1 data summary.

Mole % GaAs	Λ_3 - Λ_1 Peaks (eV)		Δ_1 (eV)	Method
0	2.524±0.003	2.791±0.009	0.267±0.009	CGE
20	2.536±0.015	2.810±0.009	0.274±0.018	CGE
44	2.562±0.006	2.822±0.015	0.260±0.015	CGE
60	2.61 ±0.01	2.84 ±0.01	0.23 ±0.01	EE
75	2.672±0.005	2.945±0.005	0.273±0.006	EE
80	2.747±0.003	2.991±0.005	0.244±0.006	CGE
80	2.709±0.005	2.971±0.005	0.262±0.006	EE
84	2.758±0.003	3.007±0.006	0.249±0.007	CGE
83	2.75 ±0.01	3.00 ±0.01	0.25 ±0.01	EE
100	2.904±0.002	3.132±0.002	0.228±0.003	CGE

for this transition. Though the form of the variation is not accurately determinable from this figure, it seems clear that it is not similar to that of Δ_0 , since the rate of change of Δ_1 with composition seems largest at the GaAs end.

There is no significant change of structural shape with composition in the case of the Λ_3 - Λ_1 as there is in the case of the fundamental edge. This fact seems to eliminate systematic changes in the surface barrier structure with composition as a source of the line-shape changes, since such surface barrier changes should produce changes in the Λ_3 - Λ_1 structure as well as in the Γ_{15} - Γ_1 structure.

The Λ_3 - Λ_1 structure in the alloys is very similar to that of the constituent compounds, indicating that compositional inhomogeneity is not a significant source of line-shape distortion. In Fig. 8 the Λ_3 - Λ_1 structures for two of the alloys are compared with those of the two compounds, demonstrating this point.

In Table III the peak energies are listed. The first large low-energy peak in Fig. 8 has been identified as the Λ_3 - Λ_1 threshold energy, and the second negative peak at higher energies is taken as the split-off threshold position. The slope change between the two peaks supports this identification, as does the absence of a significant temperature dependence of this separation. Since there are large positive and negative peaks, there

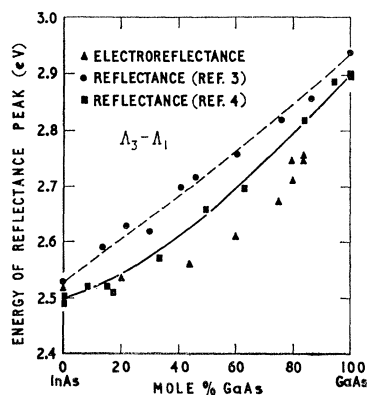


FIG. 6. Normal-incidence reflectance and electroreflectance versus composition for the Λ_3 - Λ_1 transitions.

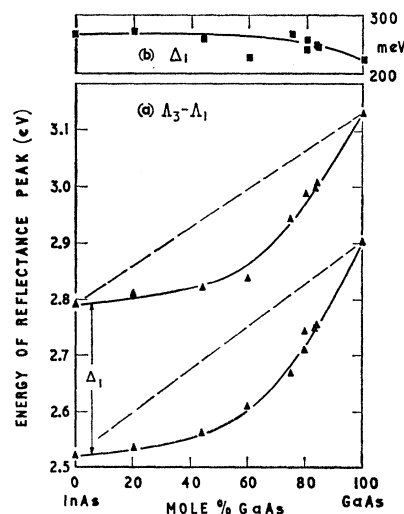


FIG. 7. The composition dependences of (a) the Λ_3 - Λ_1 transitions and (b) their spin-orbit splitting Δ_1 , measured by electroreflectance.

has been some debate about which of these peaks correspond to the Λ_3 - Λ_1 threshold. Theoretical line-shape calculations which include the effects of lifetime broadening indicate that the threshold may occur appreciably off the peak.^{44,49} A more detailed interpretation of the SBE line shape in relation to lifetime broadening effects and precise placement of the threshold relative to the structure is not practical in view of the uncertainties and inhomogeneities of the electric field.

The energy of the lowest energy peak is closer to the value found in normal-incidence reflectance for GaAs than the higher-energy peak. However, even if the higher-energy peak is chosen, or any point between, the nonlinearity shown in Figs. 6 and 7 is altered by a negligible amount. Cardona *et al.*³⁰ have pointed out that this peak is less sensitive to electric field and impurity concentration than the higher energy one, as expected from theory.^{44,49} They also point out the similarity of *sign* with the Λ_3 - Λ_1 structure of Ge, but as Seraphin³⁵ observes, this sign is dependent upon surface conditions and bulk-carrier type, and is not a convincing argument in itself.

V. IMPURITY-ASSOCIATED SPECTRA

Electroreflectance (SBE) peaks have been observed at energies less than the fundamental absorption edge and have been attributed to impurities. These show a more rapid increase in amplitude with electric field than the fundamental edge peaks, adding support to this identification.³⁵ Studies of their dependence on impurity concentration show that the peak energies increase with doping, as in the case of the Burstein shift.³⁰

⁴⁹ D. E. Aspnes, Phys. Rev. **147**, 554 (1966).

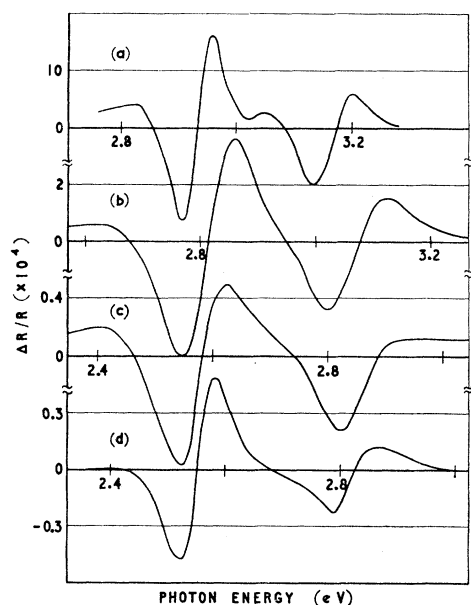


FIG. 8. A comparison of Λ_3 - A_1 SBE spectral structures for four representative samples. (a) GaAs, 1000 Ω cm p type, 200 V rms, 1 KHz, 0 V dc. (b) $\text{In}_{0.16}\text{Ga}_{0.84}\text{As}$, 425 V rms, 2.51 KHz, 0 V dc. (c) $\text{In}_{0.56}\text{Ga}_{0.44}\text{As}$, 425 V rms, 2.00 KHz, 0 V dc. (d) InAs, 300 V rms, 10 KHz, 0 V dc.

Application of an independent optical method make possible a conclusive proof of the impurity association of these peaks. Low-temperature photoluminescence (20°K) offers increased resolution and the capacity to

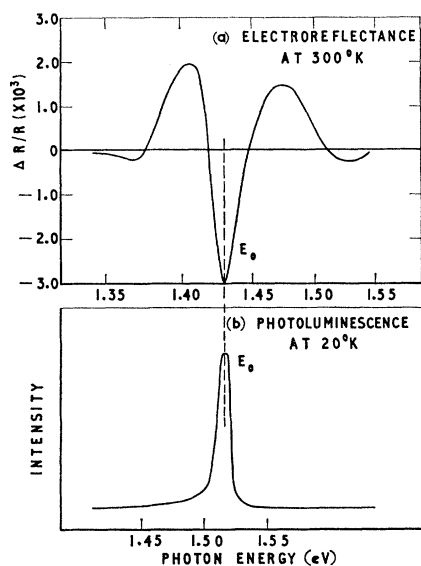


FIG. 9. A comparison of (a) electroreflectance at 300°K with (b) photoluminescence at 20°K in n -type GaAs. ($n=3 \times 10^{15}$ cm^{-3} .) The photoluminescence equipment has been described by us in a previous article [J. Appl. Phys. 38, 2547 (1967)]. In both cases an RCA-7102 photomultiplier detector was used. The energy scales of (a) and (b) have been moved so that the energy-gap peaks for the two different temperatures can be compared.

freeze out impurity states for easier detection.⁵⁰ Figure 9 shows the results of 20°K photoluminescence measurements compared with room-temperature Seraphin effect SBE measurements made on the same sample of n -type GaAs, 3×10^{15} cm^{-3} . No extra peaks are observed at energies below the fundamental edge structure, labeled E_0 , in either experiment. Note that the dashed line indicates the fundamental-edge energy at the experimental temperature according to Sturge.³⁹ Figure 10 shows a similar comparison on a sample of n -type GaAs with 2×10^{16} electrons/ cm^3 . Note the appearance of a new peak in each experiment, labeled E_I , 33 meV below the fundamental edge energy. In Fig. 11 is shown a similar comparison on n -type GaAs with 4×10^{17} electrons/ cm^3 . The peak labeled E_I is enhanced in both experiments, but in the SBE experiment it now dominates the structure, its negative swing pulling the E_0 peak across the axis. Since the samples for all these experiments were epitaxial, prepared in exactly the same way in the same reactor system and used for both experiments, it is reasonable to assume that the same defect is present in all samples, and associated with the dopant impurity. The possible identity of this defect which has been commonly observed in n -type GaAs by both electroreflectance and photoluminescence has been discussed elsewhere.⁵¹

Figure 12 shows a comparison of SBE and photoluminescence in p -type, cadmium-doped GaAs with 2×10^{18} electrons/ cm^3 . In both experiments only the cadmium acceptor level is clearly observed because of

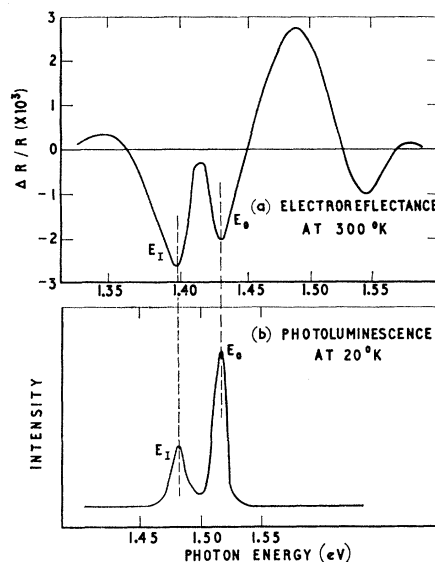


FIG. 10. A comparison like Fig. 9 in more heavily doped GaAs. ($n=2 \times 10^{16}$.) The energy scales of (a) and (b) have been moved so that the energy-gap peaks for the two different temperatures can be compared.

⁵⁰ E. W. Williams and D. M. Blacknall, Trans. Met. Soc. AIMR 239, 387 (1967).

⁵¹ E. W. Williams, Solid State Commun. 4, 585 (1966).

the high-impurity content. In the SBE experiment the change of slope indicated by the arrow marks the fundamental-edge energy, while no indication of this edge is observed in photoluminescence. Observations of SBE structure ascribed to *p*-type impurities have been reported previously.³⁰ We may conclude that SBE at 300°K is a valuable tool for detecting shallow impurities which can only be seen in other optical experiments by going to very low temperatures.

Finally we report a preliminary study of impurities in (Ga,In)As alloys. Figure 13 shows the principal (negative) peak of the fundamental-edge structure at room temperature in (In_{0.20}Ga_{0.80})As for two modulation voltage amplitudes. The 150-V curve shows a peak at 1.131 eV, while the 300-V curve shows a peak at 1.123 eV, and a shoulder at about 1.13 eV. Since impurity-associated structures vary in amplitude faster than linear,³⁵ while interband threshold structures vary about linearly in modulation voltage amplitude, this behavior is suggestive of an interband threshold ($\Gamma_{15}-\Gamma_1$) at about 1.133 eV and an impurity peak at about 1.120 eV. Figure 14 shows the same structure at 210°K compared with the 20°K photoluminescence results. This SBE structure, recorded with a 10-sec detector time constant, about 10 sec/meV scan rate and optical resolution less than 1 meV, shows three partially resolved peaks. The spacing of the high- and low-energy peaks is about 13 meV, just as was deduced from the room-temperature results. The 20°K photoluminescence results shown indicates an impurity-edge separation of about 20 meV. Additional SBE measurements at 94°K show partially resolved peaks at 1.210 and 1.191, and a small one at 1.155 eV. The latter two

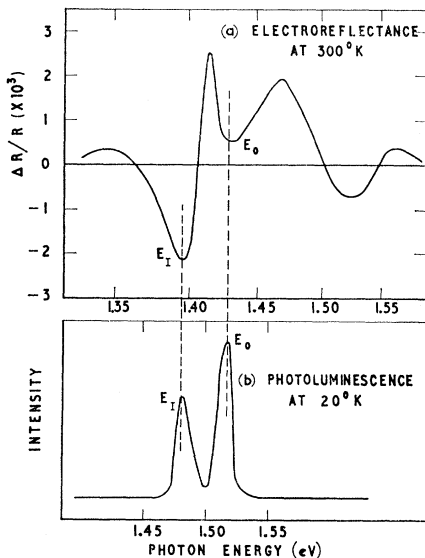


FIG. 11. A comparison like Figs. 9 and 10 in still more heavily doped GaAs. ($n=4\times 10^{17}$.) The energy scales of (a) and (b) have been moved so that the energy-gap peaks for the two different temperatures can be compared.

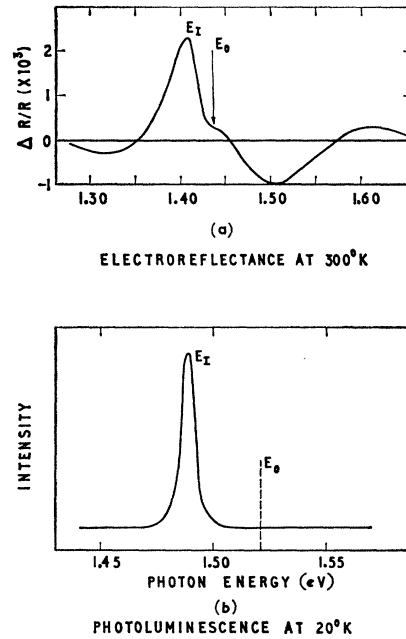


FIG. 12. A comparison as previously in very heavily cadmium doped, *p*-type GaAs. ($p=2\times 10^{18}$.) The energy scales of (a) and (b) have been moved so that the energy-gap peaks for the two different temperatures can be compared. The energy scale is larger for (b) than for (a).

show the strong voltage dependence ascribed to impurity peaks. This 19-meV separation at 94°K compares well with the 20°K photoluminescence results, but

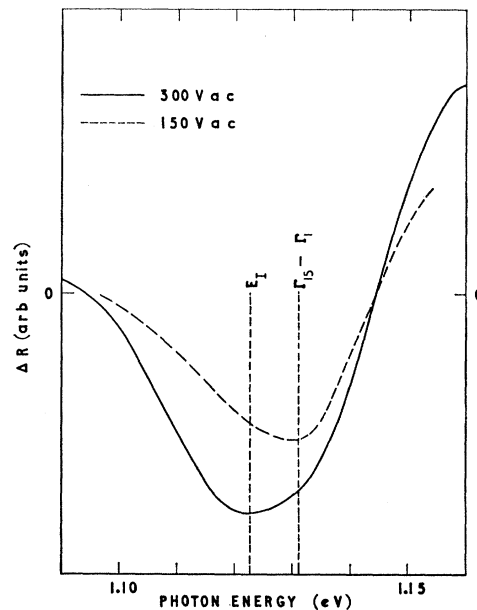


FIG. 13. The fundamental edge structure in the electroreflectance spectrum of In_{0.20}Ga_{0.80}As at room temperature for two values of modulating voltage. The positions of the edge energy and the impurity energy are indicated by the lines marked $\Gamma_{15}-\Gamma_1$ and E_I , respectively.

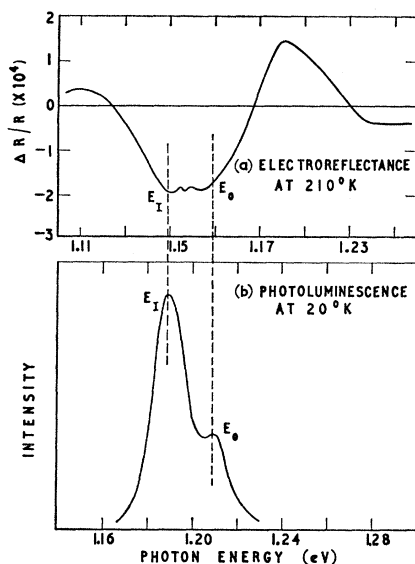


FIG. 14. Electroreflectance and photoluminescence in $\text{In}_{0.20}\text{Ga}_{0.80}\text{As}$. ($n=1 \times 10^{17}$.) The energy scales of (a) and (b) have been moved so that the energy-gap peaks for the two different temperatures can be compared.

further work is necessary to confirm the identification. Poor resolution in the photoluminescence, due to the weak intensity, made it difficult to confirm or deny the existence of further structure.

VI. DISCUSSION

A. Line Broadening

There are several possible mechanisms which may contribute to the line broadening of both the $\Gamma_{15}-\Gamma_1$ and $\Lambda_3-\Lambda_1$ electroreflectance structures.

1. Field Inhomogeneity Broadening

As was previously stated in Sec. II, both SBE techniques produce nonuniform fields. This makes it impossible to apply field-effect theory quantitatively to understand the line-shape and field dependence since the magnitude of the field gradient cannot be accurately calculated or measured. Transverse electroreflectance (TE) measurements on GaAs have shown that the field inhomogeneity produces a large broadening which varies little with temperature.³⁷ For TE, which uses a more uniform field, the linewidth of the $\Lambda_3-\Lambda_1$ series in GaAs shrinks by a factor of 3 on reducing the temperature from 300° to 90°K; but for SBE the temperature change was less than a sixth of this. The change observed for TE can be accounted for by field-effect theory, but the change is masked by the field inhomogeneity in SBE.

2. Surface and Strain Broadening

The condition of the sample surface is important in SBE. The nonuniform field is largest at the surfaces

and decreases rapidly on going into the sample bulk. Any surface effects or strain induced by polishing could be significant. The fact that little change was observed on subsequent treatments of the same sample indicated that the etching procedure successfully eliminated any severe strain effects due to mechanical polishing and that any other surface conditions were either unchanged or not detected in the SBE measurements.

3. Lifetime Broadening

The change in line shape for the $\Gamma_7-\Gamma_8$ spin-orbit split-off transitions versus composition may be explained in terms of lifetime. Since the density of states of the heavy-hole band in the region of Γ_8 does not change much from GaAs to InAs, the scattering of light holes into the heavy-hole band at a given energy will not change. However, the spin-orbit splitting $\Delta_0 = \Gamma_8-\Gamma_7$ is larger for InAs, and therefore the lifetime of the light holes at Γ_7 decreases because of the increased number of states of the heavy-hole band into which they may be scattered. This implies that the line should be broader for InAs than for GaAs.⁵² The experimental results agree with this prediction. The linewidth for InAs is $\frac{2}{3}$ times the linewidth for GaAs, and the Airy oscillations are almost completely damped by the line broadening, which appears to be Gaussian in character. Comparison of Fig. 9(a) with Fig. 5 shows this. [The spin-orbit split-off component $\Gamma_7-\Gamma_8$ is not shown in Fig. 9(a), but its shape is identical to that of $\Gamma_8-\Gamma_6$.]

Extending the above arguments to the alloys, it is to be expected that the line shape should not change until Δ_0 changes. This was found to be the case. As shown in Fig. 4(b), at the GaAs end of the alloy system no change in Δ_0 occurs and very little change in line shape was observed. When the alloy composition was less than 60-mole % GaAs a large change in line shape occurred at the same time as Δ_0 began to change.

This can also be applied to other III-V compounds. For lower energy gap materials like InSb, where Δ_0 is much greater than for InAs, the observed linewidth is approximately twice that of InAs.^{33,34} Likewise, for GaP and InP in which Δ_0 is smaller than for GaAs, the linewidth is slightly smaller than for GaAs.³⁰ This dependence on Δ_0 may be accentuated by the inhomogeneity-broadening changes which are related to E_0 and doping level.

In the case of the $\Lambda_3-\Lambda_1$ spectra there was about a factor of 2 change in broadening across the whole of the alloy system. This smaller change than for $\Gamma_{15}-\Gamma_1$ spectra indicates that, if one assumes the other broadening mechanisms equal for the two thresholds, the change in electron and heavy-hole lifetime across the

⁵² This mechanism has been successfully used to account for the broadening of the absorption edges in germanium. See T. P. McLean and E. G. S. Paige, in *Proceedings of the International Conference on the Physics of Semiconductors, Exeter, 1962* (Institute of Physics and The Physical Society, London, 1962), p. 450.

alloy system is small. A comparison of the band structures of InAs and GaAs shown in Fig. 1 shows that the differences in the density of states are small in the region where the transition takes place.

4. Alloy Broadening

In the alloys two other broadening mechanisms are possible. First, as is discussed more fully below, there is a prediction¹⁶ that a random arrangement of Ga and In on III-atom sites should produce a density of states "tail" into E_g . This would imply that the carrier lifetime and its broadening effect would change rapidly in alloys close to the compounds. The fact that there was little difference in the line shapes of the alloys with compositions close to the compounds shows that, for this particular alloy system, alloy broadening was not predominant. The Δ_3 - Δ_1 width varied by less than a factor of 2 across the entire composition range, and part of this increase in width must have been due to the higher voltages that had to be applied to obtain a signal comparable to that of the compounds. The smaller signal obtained from the alloys may be indicative of a change in the surface barrier caused by the more complex alloy surface.

Secondly, any inhomogeneity of the alloys would cause a broadening. That the alloys were in fact very homogeneous was shown by comparing the shape of the absorption edges, the Δ_3 - Δ_1 line shapes, and the x-ray measurements with those of the compounds. In every case they were similar.

5. Impurity Concentration Broadening

The different impurity compensation and doping levels in the samples will change the slope of the absorption edge to some extent.⁵³ This will in turn change the shape of the line observed in electroreflectance. That very little change in slope was observed in the absorption measurements indicates that this effect is not expected to be strong for the samples used. However, for heavily doped samples, greater than 10^{19} carriers/cc, and for closely compensated samples, line-broadening effects from this source would be expected.

Further detailed experiments are needed to ascertain which broadening mechanisms are the most important. Experiments which utilize a more homogeneous field, such as TE, would be the most useful. Studies as a function of temperature would help to eliminate some mechanisms. At the present time, however, there is a materials problem; semi-insulating InAs or (Ga,In)As alloys are not available and the TE experiments will be limited to GaAs. The technique of wavelength modulation offers another alternative.⁵⁴ Since no field is applied to the sample, its resistivity is of no consequence and the temperature dependences of broaden-

ing mechanisms which are field-independent could be measured.

Extensions of the present SBE measurements to energies below 0.45 eV with the new experimental technique that is now available⁵⁵ would also be useful. The differences between the Γ_8 - Γ_6 and Γ_7 - Γ_6 line shapes could then be studied across the whole of the alloy system and changes in hole lifetime may be observed.

B. Spin-Orbit Splitting, Δ_0 and Δ_1

Δ_0 for InAs was measured directly for the first time as 0.446 ± 0.008 eV.²⁴ This is quite close to the value of 0.43 eV estimated by Matossi and Stern⁴¹ from studies of intraband free-hole transitions. Matossi and Stern applied a technique developed for InSb by Kane.⁵⁶ It is possible that an extension of Kane's method could be used to explain the change in Δ_0 across the alloy system. Perturbation theory could be used to account for random ordering of the atoms in the alloy system. Thompson *et al.* have shown that the randomness effects appear stronger in the lower energy gap alloys than in the higher energy gap alloys,⁵⁷ suggesting an empirical relation between the energy gap and the disorder parameter C . (C is defined in Sec VI C.)

A suggestion by J. C. Phillips⁵⁸ relates the compositional change in Δ_0 with the linewidth change and adds strength to the lifetime broadening discussion above. The change in Δ_0 is related to the relative phases of either the metal and the arsenic contributions to the Γ_{15} wave functions. Thus,

$$\psi(\Gamma_{15}) = a(x)\psi_M + (x)\psi_{As},$$

where ψ_M is the virtual-crystal wave function for the metal position, and x is the concentration of Ga. The concentration dependence of Δ_0 would be influenced by the ab interference term.¹⁸ The ab and b^2 terms add near InAs and produce a greater spin-orbit splitting. Because Δ_0 is almost constant near GaAs, the b^2 and ab terms must cancel, giving a smaller Δ_0 . This compositional dependence in the wave function must be reflected in the Γ_8 and Γ_7 lifetime broadening through the interaction matrix elements. The approximate cancellation of b^2 and ab terms near GaAs implies less lifetime broadening than near InAs, where b^2 and ab terms must add.

For Δ_1 the splittings reported here for the compounds are in good agreement with those found previously from reflectance and electroreflectance measurements. The variation of Δ_1 between the compounds was small,

⁵³ C. R. Pidgeon, J. Feinleib, S. H. Groves, and R. J. Phelan, Jr., *Bull. Am. Phys. Soc.* **12**, 297 (1967).

⁵⁶ E. O. Kane, *J. Phys. Chem. Solids*, **1**, 249 (1947); C. Hilsum and A. C. Rose-Innes, *Semiconducting III-V Compounds* (Pergamon Press, Inc., Oxford, 1961), pp. 18 and 49.

⁵⁷ A. G. Thompson and J. C. Woolley, *Can. J. Phys.* **45**, 255 (1967).

⁵⁸ J. C. Phillips (private communication).

⁵³ G. Lucovsky, *Appl. Phys. Letters* **5**, 37 (1964).

⁵⁴ R. E. Drews, *Bull. Am. Phys. Soc.* **12**, 384 (1967); I. Balslev, *Phys. Rev.* **143**, 636 (1966).

approximately 40 meV in contrast to about 105 meV for Δ_0 . This reduces the accuracy with which the form of the variation of Δ_1 across the alloy system can be determined. The curve plotted through the points in Fig. 7(b) is only an estimate and may be appreciably influenced by the errors in measurement and in plotting in Fig. 7(a).

The modified $\frac{2}{3}$ spin-orbit splitting rule mentioned by Thompson *et al.* is approximately obeyed in the compounds and the (Ga,In)As alloys.¹⁰ This rule states that Δ_1 has a value of $\frac{2}{3} \Delta_0$. To our knowledge there is as yet no published theoretical derivation of this rule, so it will not be discussed further here.

C. Alloy Composition Dependence

A deviation from linearity of the $\Gamma_{15}-\Gamma_1$ and $\Lambda_3-\Delta_1$ transition energies as a function of alloy composition is predicted by the modified virtual-crystal model. This model predicts a linear variation of the energy gap with composition in first order, and a quadratic correction in second order.¹⁶ This model has been fitted to the alloy system (Ag,Cu)I for the variation of several exciton peaks.⁶⁹ More recently, it has been applied to the fundamental energy gap variation of several III-V alloy systems⁵⁷ by using quadratic composition dependence:

$$E_x = A + Bx + Cx^2.$$

Here E_x is the interband energy at a particular alloy composition x , which is the mole fraction of the compound with the largest energy gap. A is the energy gap of the compound with the smallest gap and $D = A + B + C$ is the energy gap of the largest energy-gap compound. C is equal to four times the deviation of the observed gap from linear behavior at the equimolecular composition ($x=0.5$). C represents the departure of the alloy from the virtual crystal, and is calculated assuming a random arrangement of component atoms on lattice sites.

If this equation is applied to the present data, the value of C obtained is approximately 0.6 eV for three of the four transitions, and 0.7 eV for the $\Gamma_{15}-\Gamma_1$ split-off transition $\Gamma_7-\Gamma_6$.

Cohen and Bergstresser⁶⁰ have examined the effect of the concentration dependence of the critical-point loca-

tion on the concentration dependence of $\Gamma_{15}-\Gamma_1$ and $\Lambda_3-\Delta_1$ in their pseudopotential calculation. Although their results are in the correct direction, their calculated curve deviates from a linear one by only 10–20 meV, compared to the experimental 100–200 meV.

D. Impurity Associated Spectra

The comparison of photoluminescence spectra at 20°K with electroreflectance at 300°K has proved that shallow acceptors and donors can be observed in electroreflectance spectra. When the impurities are absent in photoluminescence they are absent in electroreflectance. On increasing the impurity doping level above a certain critical value, thought to be in the region of $1 \times 10^{16}/\text{cc}$, an impurity peak is observed in both experiments which grows in intensity as the doping is further increased and dominates the spectrum when the level is above 10^{18} impurities/cc.

The observation of an impurity-associated electroreflectance response for relatively small impurity concentrations should not be surprising even though direct optical-absorption experiments require much higher concentrations for observation. Two facts are important to keep in mind: First, being a critical-point phenomenon, electroreflectance signals ordinarily represent only the small fraction of the valence band population located close to the interband critical point in k space. Hence sensitivity to small numbers of electrons is expected. Empirically the minimum reflectivity changes to which electroreflectance is sensitive are of order 10^{-6} , compared to 10^{-3} in static reflectivity experiments. Second, electroreflectance measures the *field dependence* of the reflectivity, which is quite a separate quantity from static reflectivity or absorption.

ACKNOWLEDGMENTS

The authors wish to thank R. W. Conrad for supplying most of the alloy samples, and M. L. Cohen, M. Cardona, J. C. Phillips, H. B. Bebb, T. P. McLean, and A. Lettington for helpful discussions. Some of the alloy samples were prepared as part of a research program sponsored by the U. S. Air Force Avionics Laboratory, Wright-Patterson Air Force Base, under Contract No. AF33 (615)-1272.

⁶⁰ Marvin L. Cohen and T. Bergstresser (private communication).

⁶⁹ M. Cardona, Phys. Rev. **129**, 69 (1963).